Journal of Magnetic Resonance **137,** 83–92 (1999)
Article ID jmre.1998.1669, available online at http://www.idealibrary.com on IDEAL®

Angular Variation of Electron Paramagnetic Resonance Spectrum: Simulation of a Polycrystalline EPR Spectrum

Sushil K. Misra

Physics Department, Concordia University, 1455 de Maisonneuve Boulevard West, Montreal, Quebec, H3G 1M8 Canada

Received March 18, 1998; revised November 24, 1998

A procedure based on homotopy, involving a quick calculation of EPR line positions for various orientations of the external magnetic field by the method of least-squares fitting and Taylor-series expansion, using a known line position at an infinitesimally close orientation of the external magnetic field as the initial value, by using the eigenvectors and eigenvalues of the spin-Hamiltonian matrix in single crystals, has been exploited to simulate a polycrystalline EPR spectrum. This requires rigorous calculations of intensities of resonant lines, along with their positions. Specifically, details are given of the numerical techniques involving time-efficient matrix diagonalization to obtain the eigenvalues and eigenvectors required to calculate positions and intensities of EPR lines by the method of least-squares fitting. Finally, the procedure of how to simulate a polycrystalline EPR spectrum is outlined, the required steps are listed, and illustrative examples are given.

Key Words: **simulation; powder; EPR spectrum; least-squares fitting; angular variation.**

I. INTRODUCTION

Simulation of polycrystalline (or powder; these two terms will hereafter be used interchangeably) spectrum of a transition-metal ion has been of great interest recently, especially in metalloproteins or other samples (*1*). These materials are characterized by rather large zero-field splitting (ZFS) parameter (D), for which it is often not possible to grow single crystals, and one has no choice but to analyze a powder-sample spectrum to estimate ZFS parameters. The straightforward way to simulate a powder spectrum is to use perturbation expressions if the ZFS parameters are not large or to use the brute-force technique wherein diagonalization of the spin-Hamiltonian matrix (SH) is performed to compute the required energy levels for values of the external magnetic field varied in small steps over a chosen range, referred to hereafter as brute-force matrix diagonalization (BFMD) method. This is done for selected orientations of the external magnetic field (**B** hereafter) over the unit sphere. Evidently, if the ZFS parameters are large and spin (S) of the transition-metal ion is also large, e.g., $S = \frac{5}{2}$ for the Mn^{2+} ion and $S = \frac{7}{2}$ for the Gd^{3+} ion, the brute-force technique requires exorbitant computer times. On the other hand, for large D, the perturbation approximation is not valid at orientations of **B** away from the crystal axis required to calculate a powder spectrum. Misra and Vasilopoulos (*2*) (MV hereafter) published a technique of quickly calculating angular variation of resonant EPR line positions in a single crystal by calculating EPR line positions by the method of least-squares fitting (LSF) for an orientation of **B** infinitesimally close to the one for which the resonant line position is known.

Since, as pointed out above, it is of great interest to simulate powder spectra, which requires a knowledge of spectral intensities, it is worthwhile to extend the technique of MV to calculate the intensity of a line for an orientation of the external magnetic field infinitesimally close to the one for which the eigenvectors and eigenvalues corresponding to the levels participating in resonance are known, by the LSF technique, to minimize the computer time required. (This method is referred to as "homotopy," implying continuation or embedding (*3*)). The purpose of this paper is to provide the details of how this approach, referred to hereafter as homotopy matrix diagonalization (HTMD) method, can be realized.

Details of the simulation of a powder spectrum are given in Section II. Section III deals with the LSF procedure specific to the required computation, along with some relevant helpful numerical techniques. Section IV gives the details of the computer calculation of a simulated powder spectrum. Section V includes a list of the various steps required in such a simulation, while illustrative examples are given in Section VI. Section VII is devoted to a discussion of computational times required in the BFMD, HTMD, and perturbation approaches. Discussion and concluding remarks are provided in Section VIII.

II. COMPUTATION OF POWDER SPECTRUM

The EPR spectrum in a polycrystalline material can be simulated by overlapping spectra computed for a large number of uniformly distributed orientations (θ, φ) of the external magnetic (Zeeman) field, **B,** over the unit sphere weighted by $\sin\theta d\theta d\varphi$ to take account of the distribution of the various constituting crystallites whose principal axes are orientated in the interval $d\theta$, $d\varphi$ about (θ, φ). As well, a lineshape function, $F(B_{ri}, B)$, for the various possible transitions $i' \leftrightarrow i''$ is used which could be Gaussian, Lorentzian, or a complicated func-

1090-7807/99 $30.00

tion appropriate to the sample, in addition to each line position being weighted in proportion to its transition probability. (Here B_{ri} is the ith resonant field value.)

Thus, the simulated spectrum can be expressed as

$$S(B, \nu_c) = \int_{\theta=0}^{\pi/2} \int_{\varphi=0}^{2\pi} \sum_i P(i, \theta, \varphi, \nu_c) \times F(B_{ri}, B) d(\cos\theta) d\varphi. \quad [2.1]$$

In Eq. [2.1], $P(i, \theta, \varphi, \nu_c)$ is the transition probability for the ith transition, between the levels i' and i'', participating in resonance at the microwave frequency (hereafter the term microwave radiation refers to electromagnetic waves of frequency 1–950 GHz), ν_c, at the orientation (θ, φ) of **B** over the unit sphere. It is expressed as

$$P(i, \theta, \varphi, \nu_c) \propto |\langle\Phi_{i'}|(B_{1x}S_x + B_{1y}S_y + B_{1z}S_z)|\Phi_{i''}\rangle|^2. \quad [2.2]$$

In Eq. [2.2], S_α and $B_{1\alpha}$ $(\alpha = x, y, z)$ represent the components of the electron spin operator, **S,** and the modulation RF field $\mathbf{B}_1$. $|\Phi_{i'}\rangle$ and $|\Phi_{i''}\rangle$ are the eigenvectors of the spin-Hamiltonian matrix, H, corresponding to the energy levels $E_{i'}$, and $E_{i''}$ participating in resonance $[H|\Phi_k\rangle = E_k|\Phi_k\rangle]$.

It is important to describe briefly the two alternative techniques of obtaining an EPR spectrum as they have bearing on proposed simulation of a powder spectrum.

(i) Swept-field EPR. The microwave frequency is kept fixed and the external magnetic field is swept over a chosen range. Resonance occurs when the energy difference between eigenpairs becomes equal to the energy of the microwave quantum. This way, all the transitions are recorded in an appropriate magnetic-field sweep interval. This technique has been used most frequently because of experimental convenience.

(ii) Swept-frequency EPR. The magnetic field is kept fixed and the frequency of the microwave radiation is varied over an appropriate interval so that all the transitions are recorded. It can be easily seen that this case can be taken into account for powder-spectrum simulation by using steps parallel to those presented in this paper for swept-field EPR for the simple reason that a resonance occurs when the energy difference between the eigenpairs is equal to the quantum of microwave radiation regardless of whether this condition is achieved by varying the magnetic field or by varying the frequency of microwave radiation.

It is clear from Eq. [2.1] that, in particular, one needs to know the resonant field values for the various transitions, as well as their transition probabilities. The most direct way to calculate these is to use the exorbitantly time-consuming BFMD technique, as explained above in Section I. A considerable saving of computer time can be accomplished if one uses the HTMD technique to minimize the number of diagonalizations of the SH matrix by using the LSF technique of MV [2]. However, their efforts were confined only to the calculation of angular variation of the resonant field positions, $B_r(i, \theta, \varphi)$, in single crystals and not to the simulation of powder spectra requiring the intensities of the transitions, which, in turn, depend upon the eigenvectors $|\Phi_k\rangle$.

III. LEAST-SQUARES FITTING (HTMD) PROCEDURE AS APPLIED TO THE SIMULATION OF POWDER SPECTRA BY VARYING THE ORIENTATION OF B IN INFINITESIMAL STEPS

The simulated spectrum is computed by the use of Eq. [2.1], wherein the integrals are converted to discrete sums. The various parameters/techniques required in the computation are described below.

Resonant line positions. The procedure to calculate the resonant line position at the orientation, $(\theta + \delta\theta, \varphi + \delta\varphi)$, from the knowledge of the line position at the orientation (θ, φ), using the least-squares fitting technique and Taylor-series expansion, is

$$B_r(i, \theta + \delta\theta, \varphi + \delta\varphi, \nu_c) = \text{Iterative limit of} \left[-\left(\frac{\partial^2 S}{\partial B^2}\right)^{-1}_{B_r'} \left(\frac{\partial S}{\partial B}\right)_{B_r'} \right]. \quad [3.1]$$

In Eq. [3.1], one starts with $B_r' = B_r(i, \theta, \varphi, \nu_c)$, and S is defined as

$$S \equiv (|E_{i'} - E_{i''}| - h\nu_c)^2, \quad [3.2]$$

where h is Planck's constant and $E_{i'}$, $E_{i''}$ are the energies of the levels participating in resonance.

The procedure of how to calculate the square bracket in Eq. [3.1] numerically, using the eigenvectors and eigenvalues of the SH matrix, is described in Appendix I.

Transition probabilities. To simulate a polycrystalline spectrum, one needs to calculate the transition probabilities $P(i, \theta, \varphi, \nu_c)$ for the various transitions, given by Eq. [2.2], at various orientations of the external magnetic field, which, in turn, depend upon the eigenvectors $|\Phi_i(\theta, \varphi)\rangle$; $i = i', i''$ corresponding to the energy levels $E_{i'}$ and $E_{i''}$ participating in resonance, referred to hereafter as eigenpairs. The transition probability at the infinitesimal orientation $\theta + \delta\theta$ and $\varphi + \delta\varphi$ of **B** can be obtained from the eigenvectors $|\Phi_i(\theta + \delta\theta, \varphi + \delta\varphi)\rangle$. The latter are already computed in the final iteration to calculate $B_r(i, \theta + \delta\theta, \varphi + \delta\varphi)$ as obtained using Eq. [3.1]. The procedure for a numerical calculation of intensity for the general case when the elements of the SH matrix are complex is given in Appendix II.

Frequency/field conversion in relation to transition probability. The transition probability depends upon the eigenvectors corresponding to the eigenpairs for resonance, which de-

pend, in turn, on both the external magnetic field and the frequency of the electromagnetic radiation. In swept-field EPR, they are calculated at the resonant field, B_r, which, in turn, depends upon the microwave frequency so that the difference in the energies of eigenpairs is equal to a quantum of microwave radiation. On the other hand, in swept-frequency EPR the role of B_r is played by the fixed magnetic-field value, B_0, while the microwave frequency is made equal to the energy difference between the eigenpairs. Finally, in the simulation of a powder spectrum, a Gaussian distribution function $\{\exp[(B - B_r)^2/\sigma_B^2]\}$ is used for swept-field EPR, where ν_B and σ_B are the resonant frequency and the corresponding Gaussian width in field units, respectively, to take into account the finite width of the energy levels for each transition, as presented in this paper. On the other hand, for swept-frequency EPR this distribution assumes the corresponding form, $\exp[(\nu - \nu_r)^2/\sigma_\nu^2]$, where ν_r and σ_ν are the resonant frequency and the Gaussian width in frequency units, respectively. These distribution functions then multiply the transition probability at B_r or ν_r as given by Eq. [2.2].

IV. CALCULATION OF A SIMULATED SPECTRUM

In order to simulate a powder spectrum, $S(B, \nu_c)$, one needs to perform summations in discrete steps on a computer to calculate the integrals in Eq. [2.1]. The required specializations to enable computer simulation are described below.

Integrals. The integral in Eq. [2.1] can be expressed as a sum over different orientations (θ_j, φ_j) of **B** distributed uniformly over the unit sphere divided into grids whose intersections for successive grids are infinitesimally close to each other and over the values of **B** divided into channels, B_k, distributed over the magnetic-field interval under study. Thus, Eq. [2.1] can be expressed, using a constant C, as

$$S(B, \nu_c) = C \sum_{i,\theta_j,\varphi_j,k} P(i, \theta_j, \varphi_j, \nu_c) \times F(B_r(i, \theta_j, \varphi_j, \nu_c), B_k)\sin\theta_j. \quad [4.1]$$

In Eq. [4.1], the values of θ_j are distributed over the interval 0 to $\pi/2$, while those of φ_j are over 0 to 2π, taking into account the fact that the EPR spectrum remains unchanged when the magnetic-field orientation is reversed in direction due to time-reversal invariance, and $\sin\theta_j$ takes into account the uniform distribution of the crystallites constituting the powder such that the number of crystallites with their axes along θ_j is proportional to $\sin\theta_j$. The choice of (θ_j, φ_j) grid will be described below. The summation over k takes into account the probability of the amplitude of absorption at the magnetic-field value B_k due to the lineshape distribution $F(B_r(i, \theta_j, \varphi_j, \nu_c), B_k)$ for the ith transition for the orientation of B along the (θ_j, φ_j) direction.

(θ_j, φ_j) grid. One can conveniently choose a (θ_j, φ_j) grid where the θ value is changed from 0 to $\pi/2$ in n_θ steps where n_θ is a sufficiently large number, say $n_\theta = 300$ (i.e., at every $\frac{3}{10}$ of a degree), depending upon the convergence rate of $B_r(i, \theta_j, \varphi_j, \nu_c)$ values computed using Eq. [3.1]. Similar considerations apply to changes in φ values in n_φ steps, say $n_\varphi = 90$ (i.e., every 4 degrees), over 0 to 2π. Thus, one can start at $\theta = 0°$, $\varphi = 0°$. Then increase θ by $\pi/2n_\theta$ and compute the resonant fields $B_r(i, \theta_j, \varphi_j, \nu_c)$ and the corresponding transition probabilities $P(i, \theta_j, \varphi_j, \nu_c)$ for φ values incrementing from $\varphi = 0°$ in $2\pi/n_\varphi$ steps. The interval between successive (θ_j, φ_j) values should be chosen to be sufficiently small such that the resonant field values at these two orientations of **B** do not differ from each other by relatively large magnitudes. The various (θ_j, φ_j) values required in the sum in Eq. [4.1] are thus taken into account by the grid structure.

A quick way to take into account the weighting factor of $\sin\theta_j$ in Eq. [4.1], as followed here, is by varying $\cos\theta$ values from 0 to $\pi/2$ in n equal steps, where n is sufficiently large, such that $\cos\theta = (i - 1)/(n - 1)$ with $i = 1, 2, 3, \ldots, n$. Then the $\Delta\theta$ interval corresponding to $\Delta(\cos\theta)$ interval is $\Delta\theta = \Delta(\cos\theta)/|d(\cos\theta)/d\theta)|$. Thus, the number of θ values considered in the interval $\Delta(\cos\theta)$ is proportional to $1/\Delta\theta$, or equivalently, to $\sin\theta$.

When there appear "crossing" or "looping" transitions, e.g., in the case of the Fe^{3+} ion (*2*), problems arise when two transitions cross each other between two successive (θ_j, φ_j) values considered (crossing transition) or a transition does not occur at the adjacent (θ_j, φ_j) values (looping transition). In order to overcome these problems, certain strategies must be employed which are discussed in Appendix II. In addition, an improved partitioning scheme of the grid may be used. To this end, Wang and Hanson (*4, 5*) developed a novel scheme, named the SOPHE (Sydney Opera House) partitioning scheme, involving a combination of cubic spline and linear interpolations; the unit sphere is partitioned into triangularly shaped convexes subtending nearly the same solid angles. These publications (*4, 5*) also provide reference to earlier proposed partitioning schemes, e.g., the Igloo method for partitioning an octant of the unit sphere (*6*).

Eigenpairs participating in resonance. It is clear that the same eigenpairs which belong to the levels characterized by the electronic magnetic quantum numbers M and $M - 1$, which describe the eigenvectors of H_{Ze}, the Zeeman part of the spin Hamiltonian, should be used for the calculation of the resonant fields corresponding to allowed fine-structure transitions as the orientation (θ, φ) of **B** is changed successively to the next infinitesimally close orientation $(\theta + \delta\theta, \varphi + \delta\varphi)$ to cover the unit sphere. This is accomplished by first finding the eigenvalues and eigenvectors of H_{Ze}. The eigenvalues are then arranged, either in increasing or in decreasing order, characterized by M, the magnetic quantum number. (In the computational procedure followed in this paper this is accomplished by the use of an appropriate subroutine.) It is followed by transforming the matrix of H_{ZFS}, the zero-field part of the spin Hamiltonian by the matrix V, formed by the eigenvectors

of H_{Ze} as columns. (Of course, H_{Ze} is diagonal in this representation with the diagonal elements being the eigenvalues of H_{Ze}). The transformed spin-Hamiltonian matrix $H^T = V(H_{Ze} + H_{ZFS})V^\dagger$, so obtained in the basis of eigenvectors of H_{Ze}, is then diagonalized to find its eigenvalues and eigenvectors. This time no ordering of eigenvalues is carried out. In this manner, one is always certain that the eigenpairs characterized by M, $M - 1$, always remain the same in the homotopy procedure. Without this practice, it is frequently impossible to follow the same eigenpairs for a given transition as the orientation of **B** is changed, particularly when this orientation is not close to the principal axis of the crystal. It is noted that the M, $M - 1$, eigenpairs are, indeed, unequivocally identified when perturbation expressions are used with the electronic Zeeman term being chosen to be the zero-order term (*8*). Alternatively, since the M, M-1 eigenpair is unequivocally identified when the perturbation expressions are used, and H_{Ze} is chosen as the zero-order term, one can make a correspondence between the eigenvalues of the full Hamiltonian ($H_{Ze} + H_{ZFS}$) as obtained by matrix diagonalization and those calculated by perturbation, in which case the label M is well defined. This is done by finding the closest perturbation eigenvalues to the eigenvalues calculated by matrix diagonalization, the two sets not being identically the same.

Lineshape function $F(B_r(i, \theta_j, \varphi_j), B_k)$. The spectrum is then calculated by performing the sum in Eq. [4.1] with $P(i, \theta_j, \varphi_j)$ centered at $B_r(i, \theta_j, \varphi_j, \nu_c)$ with the lineshape function $F(B_r(i, \theta_j, \varphi_j, \nu_c)B_k)$ extended over a reasonable magnetic-field interval $\pm\Delta B$ about $B_r(i, \theta_j, \varphi_j, \nu_c)$, characteristic of the lineshape. The most commonly used lineshapes are Gaussian and Lorentzian. In particular, the Lorentzian lineshape will be used in the computations presented in this paper. For use in the summation in Eq. [4.1], it is expressed as

$$F_L(B_r(i, \theta_j, \varphi_j, \nu_c), B_k) = K_L\Gamma[\Gamma^2 + (B_k - B_r(i, \theta_j, \varphi_j, \nu_c))^2]^{-1}, \quad [4.2]$$

where Γ is the Lorentzian linewidth (half-width at half-maximum, HWHM $= \sqrt{3}\Delta B_{pp}/2$, with ΔB_{pp} being the peak-to-peak first-derivative linewidth), and K_L is a constant.

More complicated lineshapes appropriate to polycrystalline samples are discussed by Misra (*7*), and in the references given therein.

V. A LISTING OF THE VARIOUS STEPS REQUIRED IN SIMULATION OF POWDER SPECTRUM IN INFINITESIMAL STEPS BY THE USE OF LSF (HTMD) TECHNIQUE

The following steps are recommended to simulate a powder spectrum using the proposed homotopy method.

(i) The allowed resonance fields ($|\Delta M| = 1$) to be used as initial values are calculated at $\theta = \varphi = 0°$ using the third-order perturbation expressions or BFMD method for the eigenvalues E(M), (*8, 9*) and the resonance condition

$$h\nu = |E(M) - E(M - 1)|. \quad [5.1]$$

(ii) Using the resonance fields obtained for $\theta = \varphi = 0$ in step (i) as initial values, the resonance fields at $\theta = \pi/2n_\theta$, $\varphi = 0$, are then calculated by the application of Eq. [3.1], abandoning the iteration procedure when the difference of the resonance field estimated in an iteration becomes less than a small value, say 0.001 mT, from that estimated in the previous iteration. (Only $\varphi = 0$ is needed for $\theta = 0$, since for this orientation the x and y components of **B** are identically zero.) The required eigenvalues and eigenvectors of the spin-Hamiltonian matrix are computed by the use of the subroutine JACOBI, which diagonalizes real symmetric matrices and is particularly efficient when the off-diagonal elements in the SH matrix are infinitesimally small as is naturally the case in homotopy. (Briefly, the diagonalization in the JACOBI algorithm is accomplished by successive rotations to annihilate the off-diagonal elements of the 2×2 submatrix constituted by the largest off-diagonal element and the corresponding diagonal elements of the SH matrix at any stage of successive rotations. For details, see (*10*).) The B_r values obtained at $\theta = \pi/2n_\theta$, $\varphi = 0$, are then used as initial values for calculating resonance fields at $\theta = \pi/2n_\theta$ and $\varphi = 2\pi/n_\varphi$. Next, the resonance fields are calculated using Eq. [3.1] for $\theta = \pi/2n_\theta$, $\varphi = (2\pi/n_\varphi)i$, for i taking successively the values 2, 3, . . . , $n_\varphi - 1$ so as to span the φ interval over 360° in equal steps of $2\pi/n_\varphi$, using the set of resonant field values obtained in the preceding calculation as initial values. The resonance fields are then calculated for $\theta = 2(\pi/2n_\theta)$, $\varphi = 0$, using those calculated for $\theta = \pi/2n_\theta$, $\varphi = 0$, as initial values. Thereafter, the resonance fields are calculated in the same way as that for $\theta = \pi/2n_\theta$ and $\varphi \neq 0$ for $\theta = 2(\pi/2n_\theta)$ and for $\varphi = (2\pi/n_\varphi)i$ for i taking on successively the values 2, 3, . . . , $n_\varphi - 1$. These calculations are repeated by increasing θ value in steps of $\pi/2n_\theta$, and for each new θ value, with $\varphi = 0$ the B_r values as calculated for the previous θ value with $\varphi = 0$ are used as initial values to calculate new B_r values. In total, the resonance fields are calculated for θ values in steps of $\pi/2n_\theta$ from 0 to $\pi/2$, and for each θ value appropriate φ values are chosen in steps of $2\pi/n_\varphi$ to cover the interval of 0 to 2π. For the resonance fields so calculated at each orientation (θ_j, φ_j) of **B,** the corresponding relative intensity of the $i' \leftrightarrow i''$ transition, $P(i, \theta, \varphi, \nu_c)$, is also calculated by the use of Eq. [2.2]. The numerical technique used to accomplish this is described in Appendix II. The resonance fields for the various transitions and the corresponding intensities for various (θ_j, φ_j) combinations are then stored, to be used later for simulation of powder spectrum. (It is noted that a practical way to automatically ensure the inclusion of the weight factor of sin θ is by varying cos θ uniformly over the interval 1 to 0 as described in Section III above).

(iii) The magnetic-field range over which the spectrum is to

be simulated is divided into equally spaced points, B_k referred to as channels (k); e.g., into 8000 channels. Each resonance field is then changed, if necessary, to assume the value of the closest channel, and the intensity of that resonance field, as given by Eq. [2.2], is assigned to be the y value at that channel, with the channel representing the x value. All resonance fields are thus taken into account. The lineshape distribution is, thereafter, incorporated by distributing the intensity about a channel corresponding to a resonance line according to the lineshape function centered at that channel over a reasonably large interval ΔB, e.g., 0.5 T, on both the higher and the lower field sides of B_r. (In general, $\Delta B = \pm\Delta B_{1/2}$ for good precision for Lorentzian lineshape, where $\Delta B_{1/2}$ is the full-width at half-maximum, FWHM.) Channel intensities corresponding to all the resonance fields calculated for the various (θ_j, φ_j) values are thus taken into account by extending the minimum field of the range, $B_{\min}$, to $B_{\min} - \Delta B$ and the maximum field of the range, $B_{\max}$, to $B_{\max} + \Delta B$. The simulated absorption spectrum, $S(B, \nu_c)$, is calculated in this manner.

(iv) Usually, it is the first derivative of the absorbed microwave power that is experimentally measured. The simulated first-derivative spectrum is calculated by taking the derivative with respect to B of $S(B, \nu_c)$, as given by Eq. [4.1], along with that of the lineshape. Specifically, for the Lorentzian lineshape, given Eq. [4.2], one has for the first derivative

$$\partial F_L(B_r(i, \theta_j, \varphi_j, \nu_c), B_k)/\partial B_k = -2K_L\Gamma[\Gamma^2 + (B_k - B_{ri})^2]^{-2}(B_k - B_{ri}). \quad [5.2]$$

In Eq. (5.2), and hereafter, B_{ri} stands for $B_r(i, \theta_j, \varphi_j, \nu_c)$. Thus, the simulated first-derivative absorption spectrum is expressed, from Eq. [4.1], as

$$\partial S(B, \nu_c)/\partial B_k = C \sum_{i,\theta_j,\varphi_j,k} P(i, \theta_j, \varphi_j), \partial F_L(\omega_i, B_r(i, \theta_j, \varphi_j), B_k)/\partial B_k \sin\theta_j \quad [5.3]$$

$$= N \sum_{i,k} |\langle\Phi_{i'}|B_{1x}S_x + B_{1y}S_y + B_{1z}S_z|\Phi_{i''}\rangle|^2 \times (B_k - B_{ri})[\Gamma^2 + (B_k - B_{ri})^2]^{-2}. \quad [5.4]$$

In Eq. [5.4], the constant, N, may be appropriately chosen, e.g., the calculated value with the largest magnitude of the y value of all the channels was here set equal to 1.

VI. ILLUSTRATIVE EXAMPLE

The proposed homotopy technique will now be illustrated by application to the case of $Mn(\gamma\text{-picoline})_4I_2$ powder sample, characterized by a rather large value of the zero-field splitting parameter, D, as measured by Lynch *et al.* (*8*) at 249.9 GHz (far infrared), who simulated the spectrum using third-order perturbation expressions for the energy (*8, 9*) and the same zero-order relative intensity ($|\langle M, m|S_+ + S_-|M', m\rangle|^2$) = $[S(S + 1) - M(M + 1)]$ (*8*) of the various $M \leftrightarrow M'$ "allowed" fine-structure ($M' = M - 1$) transitions independent of the orientation of the external magnetic field with respect to the axis of the various crystallites constituting the powder. (Here M is the magnetic quantum number and S is the electron spin with $S_+ = S_x + iS_y$ and $S_- = S_x - iS_y$ the raising and lowering operators, respectively.

The spectrum observed by Lynch *et al.* (*8*) did not exhibit any hyperfine structure, and the magnetic field was swept from 4.4–9.4 T. Thus, only the fine structure will be taken into account here in the simulated spectrum. The following spin-Hamiltonian was used (*8*):

$$H = g\mu_B B(S_z\cos\theta + S_x\sin\theta\cos\varphi + S_y\sin\theta\sin\varphi) + D[S_z^2 - S(S + 1)/3] + E(S_x^2 - S_y^2). \quad [6.1]$$

In Eq. [6.1], $g = 2.000$ for Mn^{2+}; μ_B is the Bohr magneton, $D/g\mu_B = 1.0728$ T and $E/g\mu_B = 10$ mT are the zero-field splitting parameters (*8*), and the (x, y, z) axes define the coordinate system used. (In spherical coordinate system, $z = r\cos\theta$, $x = r\sin\theta\cos\varphi$, $y = r\sin\theta\sin\varphi$.) The fourth-order spin-operator terms in the spin Hamiltonian, having negligible effect at 249.9 GHz, were not taken into account. (The D and E values chosen here are slightly different from those used in Ref. (*8*), as the ones chosen here provide a better fit to the experimental spectrum.)

The simulated first-derivative powder EPR spectrum as expressed by Eq. [5.3], using a Lorentzian lineshape with the HWHM (ΔW) value of 70 mT characterized by the lineshape function given by Eq. [4.3], as well as that calculated using third-order perturbation approximation at 249.9 GHz (far infrared) (*10*), is exhibited in Fig. 1. Figure 2 shows the spectrum simulated by the HTMD method along with the experimental spectrum (*8*) in the 4.4–9.0 T range. The powder spectrum as simulated by HTMD method at 95 GHz (W band) is given in Fig. 3, which also includes for comparison the spectrum simulated using third-order perturbation expressions. From Figs. 1 and 3, it is clear that simulation with the HTMD method is significantly different from that accomplished by the use of perturbation approximation, especially at 95 GHz where the perturbation approximation is much less valid compared to that at 249.9 GHz because of large D.

VII. COMPUTATIONAL TIME: BRUTE-FORCE MATRIX DIAGONALIZATION VERSUS HOMOTOPY MATRIX DIAGONALIZATION

It is profitable to examine the computer-time economies achieved when powder spectra are simulated using the homotopy technique. In a BFMD procedure, the SH matrix is diagonalized at each orientation of **B** at small intervals, e.g., every 5 mT, over the magnetic-field range and eigenpairs are found by comparing the energy differences between the various energy levels to be closest to the energy of a quantum of

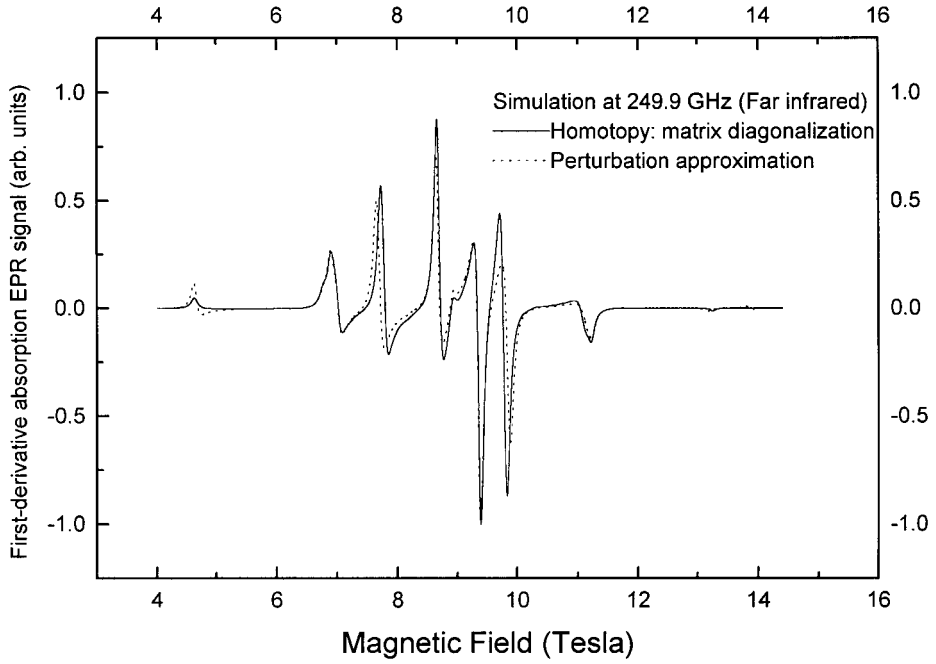

FIG. 1. Powder spectra for Mn^{2+} in $Mn(\gamma\text{-picoline})_4I_2$ at 249.9 GHz (far infrared) with $g = 2.000$, $D/g\mu_B = 1.0728$ *T*, $E/g\mu_B = 10$ mT with the spin-Hamiltonian described by Eq. [6.1] as simulated both by the use of the HTMD method and by third-order perturbation expressions.

microwave radiation. The process must be further refined over smaller magnetic-field intervals for the various transitions to determine the initial resonance fields, B_r. Thus, for the example considered in this paper covering the *B*-field interval from 4 to 14 T, if diagonalizations were performed in 5-mT steps then 2000 diagonalizations of the SH matrix are required. This might also involve another factor of 50 for the five allowed transitions if smaller steps are also included, since each tran-

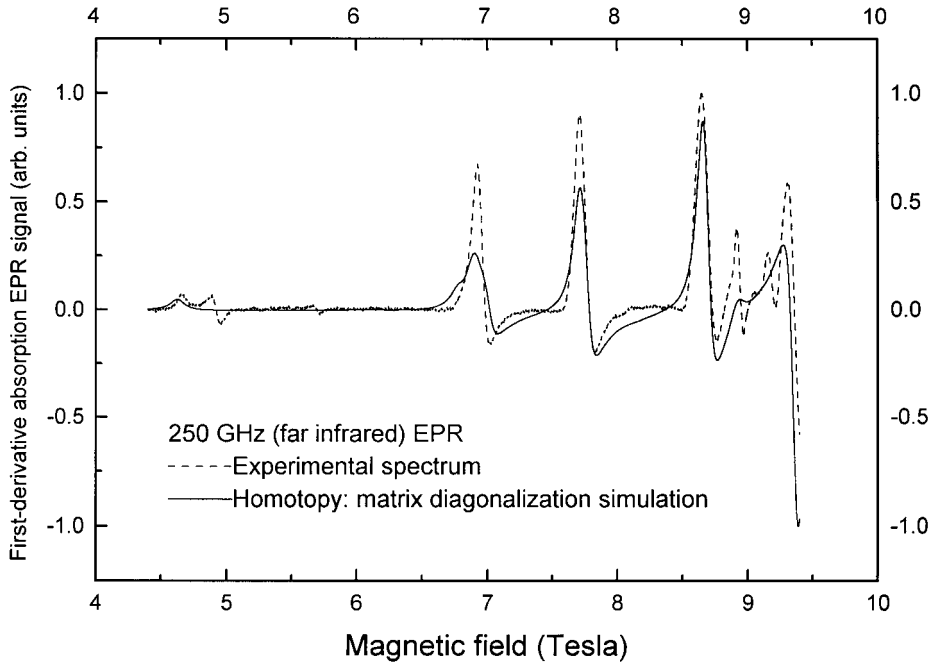

FIG. 2. Powder spectrum for Mn^{2+} in $Mn(\gamma\text{-picoline})_4I_2$ at 249.9 GHz (far infrared) with $g = 2.000$, $D/g\mu_B = 1.0728$ T, $E/g\mu_B = 10$ mT with the spin-Hamiltonian described by Eq. [6.1] as simulated by the use of the HTMD method, plotted along with the one experimentally measured in the range 4.4–9.4 T. (The magnetic field could not exceed 9.4 T experimentally.) It is noted that the experimental peaks that do not correspond to those in the simulated spectrum belong to another unknown impurity that is present rather than to the Mn^{2+} ion (*8*).

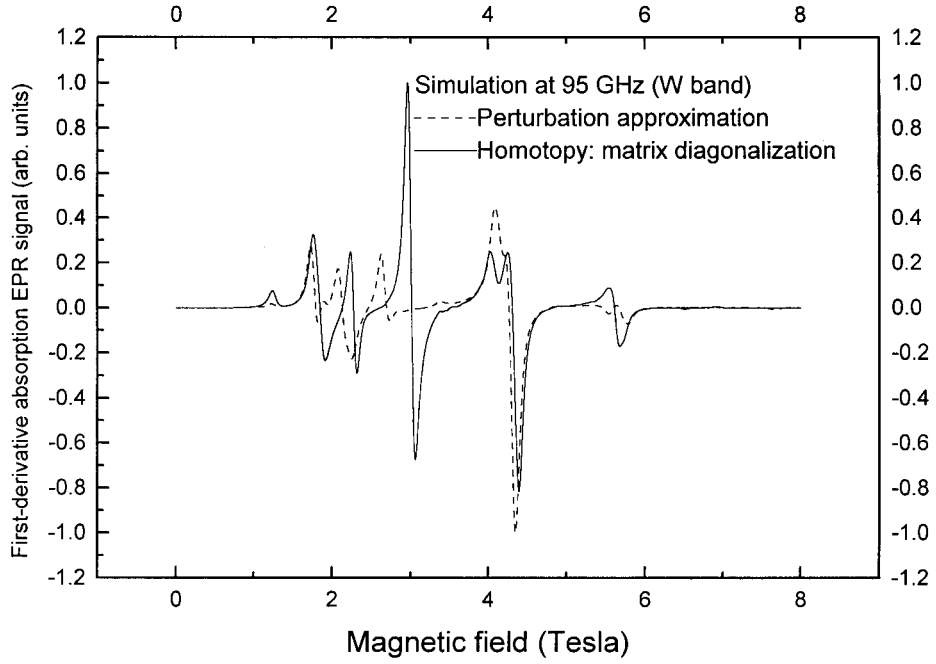

FIG. 3. Same details as in the legend to Fig. 1, except that the frequency is 95 GHz (W band). (There is no experimental spectrum available for comparison.)

sition requires 10 diagonalizations. Consequently 10^5 more diagonalizations are required for each orientation of **B** to estimate the initial values of B_r to be refined further by the use of Eq. [3.1] in the BFMD approach than those required in the HTMD technique, since in the latter the initial B_r values require no computation as they have already been calculated for the previous infinitesimally close orientation of **B.** Consequently, it is estimated that the BFMD method requires five orders of magnitude more diagonalizations, or a correspondingly longer computational time than that required in the HTMD method. No attempt has here been made to carry out a BFMD simulation because of the exorbitant estimated computational time involved. In the example presented in this paper (Fig. 1) it took 4 h 9 min 1.77 s on the powerful IBM RS/6000 Unix computer at the Cornell University Theory Center to simulate the spectrum by the HTMD method when a grid, which consisted of 300 θ values and 90 ϕ values for each θ value, was used. (It should be mentioned that the SH matrix to be diagonalized using the JACOBI subroutine was of 12×12 dimension, since this subroutine diagonalizes only a real matrix. The imaginary part is thus handled using the procedure described in (*10*), requiring diagonalization of a matrix of twice the dimension of that of the SH matrix.)

It is noted that the matrix-diagonalization procedure is capable of handling any SH matrix, even if the off-diagonal terms are sufficiently large to invalidate the use of perturbation technique. As well, it is applicable to any values of the electron and nuclear spins. Further, although it is desirable to use the HTMD technique to simulate a polycrystalline spectrum rigorously, it should not be forgotten that the perturbation approach is useful when it is valid and when one is not interested in simulating a polycrystalline spectrum quantitatively. In this case, a qualitative spectrum can be simulated quickly since perturbation expressions do not require time-consuming matrix diagonalization, and the calculation of a resonant field using the resonance condition, Eq. [5.1], and eigenvalues can be readily accomplished by Newton–Raphson method as described in Numerical Recipes (*10*). Using this approach the above example requires only 7 s of computational time to simulate the spectrum on the IBM RS/6000 computer at Cornell University Theory Center.

VIII. DISCUSSION AND CONCLUDING REMARKS

The procedure of simulating a powder spectrum as outlined in this article using the technique of homotopy and numerical diagonalization of the spin-Hamiltonian matrix is rigorous, since eigenvalues and eigenvectors of the SH matrix are used rather than perturbation expressions. This is particularly useful when the zero-field splitting parameter, D, is relatively large, in which case for smaller microwave frequencies, e.g., 95-GHz (W band) perturbation approximation is not justified in the example considered here: $D/h\nu \sim 0.1$ at 249.9 GHz, while $D/h\nu \sim 0.25$ at 95 GHz. The proposed HTMD procedure, using JACOBI diagonalization algorithm, is particularly efficient in computer time required when the off-diagonal terms of SH matrix at successive orientations of **B** are naturally infinitesimally small in homotopy. The simple (θ_j, φ_j) grid over the unit sphere as suggested here may be replaced by more efficient partitioning techniques, e.g., the SOPHE grid described by Wang and Hanson (*4, 5*) or the Igloo method (*6*).

The procedure illustrated in this paper can be easily ex-

tended to simulate powder spectra for electron nuclear double resonance, solid-state nuclear magnetic resonance, nuclear quadrupole resonance, and electron spin echo envelope modulation, as well as to include hyperfine structure, if there is any.

Finally, it is noted that the (θ_j, φ_j) grid as chosen here is quite appropriate for the Mn^{2+} ion, since there are no "looping," or "lobe," transitions (*2*). However, when these exist, e.g., in the case of the Fe^{3+} ion, certain strategies are required, and a relevant discussion is provided here in Appendix II. In addition, a superior partitioning scheme (*4–6*) may be exploited to advantage, among other things, to this end.

It is worthwhile to emphasize that if one can calculate the EPR line positions' angular variation for an external magnetic field orientations over the unit sphere by homotopy for a single crystal, as, for example, in (*2*), then the simulation of powder spectrum is readily accomplished by following the procedure described in this paper. Thus, it is clear that the cases involving looping or lobe transitions and allowed hyperfine transitions ($\Delta m = 0$, m being the nuclear magnetic quantum number) can clearly be handled by this technique, since single-crystal angular variation of resonant line positions for these cases were already considered in (*2*). The extension of this technique to the cases involving both forbidden fine ($\Delta M = \pm 2, \pm 3, \pm 4, \ldots$) and forbidden hyperfine ($\Delta m = \pm 1, \pm 2, \pm 3, \ldots$), as well as superhyperfine, transitions can also be made by first calculating the EPR line positions' angular variation for a single crystal. Consequently, no examples of these cases are given in this paper, since its objective is to outline the methodology and not to provide an encyclopedic collection of examples.

The simulation procedure presented here, among others, is eminently amenable to be exploited for estimation of spin-Hamiltonian parameters from a powder spectrum by the least-squares fitting procedure and numerical diagonalization of the spin-Hamiltonian matrix similar to that proposed in (*11*) in context with single-crystal EPR spectra, even though the powder spectrum possesses further complications over and above those of a single-crystal EPR spectrum. This LSF technique will, thus, be of immense help to this end, especially in those cases where single-crystal samples cannot be prepared, e.g., transition-metal ions doped metalloproteins. Efforts are currently in progress by the author to accomplish this.

APPENDIX I

Evaluation of the Right-hand Side of Eq. [3.1]

From the definition of S, as given by Eq. [3.2], one obtains

$$\frac{\partial S}{\partial B} = 2(|E_{i'} - E_{i''}| - h\nu_c)\left(\frac{\partial E_{i'}}{\partial B} - \frac{\partial E_{i''}}{\partial B}\right) \text{sign}(E_{i'} - E_{i''}), \quad [I.1]$$

where

$$\text{sign}(E_{i'} - E_{i''}) = \frac{(E_{i'} - E_{i''})}{|E_{i'} - E_{i''}|}.$$

In Eq. [I.1], the derivative of an eigenvalue $E_{i'}$ or $E_{i''}$ can be evaluated by the use of Feyman's theorem (*12*), e.g.,

$$\begin{aligned}\frac{\partial E_{i'}}{\partial B} &= \left\langle \Phi_{i'} \left| \frac{\partial H}{\partial B} \right| \Phi_{i'} \right\rangle \\ &= \mu_B \langle \Phi_{i'} | g_{zz} \cos\theta S_z + g_{xx} \sin\theta \cos\varphi S_x \\ &\quad + g_{yy} \sin\theta \sin\varphi S_y | \Phi_{i''} \rangle, \end{aligned} \quad [I.2]$$

where μ_B is the Bohr magneton; $g_{\alpha\alpha} (\alpha = x, y, z)$ are the components of the $\tilde{\mathbf{g}}$ tensor. (It has been assumed that the $\tilde{\mathbf{g}}$ tensor is diagonal in the coordinate axes chosen here.) In writing Eq. [I.2], the fact that only the Zeeman term,

$$H_Z = \mu_B \mathbf{S} \cdot \tilde{\mathbf{g}} \cdot \mathbf{B}, \quad [I.3]$$

depends on the external field has been taken into account, and $B_z = B \cos\theta$, $B_x = B \sin\theta \cos\varphi$, $B_y = B \sin\theta \sin\varphi$. From Eq. [I.2], one obtains, ignoring the second derivatives because of the infinitesimally close orientation of $\mathbf{B}$ from the previous orientation,

$$\frac{\partial^2 S}{\partial B^2} = 2\left(\frac{\partial E_{i'}}{\partial B} - \frac{\partial E_{i''}}{\partial B}\right)^2. \quad [I.4]$$

Thus, to be used in Eq. [3.1],

$$\begin{aligned} -\left(\frac{\partial^2 S}{\partial B^2}\right)^{-1}\left(\frac{\partial S}{\partial B}\right) &= -(|E_{i'} - E_{i''}| - h\nu_c) \\ &\quad \text{sign}(E_{i'} - E_{i''}) / \left(\frac{\partial E_{i'}}{\partial B} - \frac{\partial E_{i''}}{\partial B}\right). \end{aligned} \quad [I.5]$$

APPENDIX II

Calculation of Intensities of Lines

The intensity $P(i, \theta, \varphi)$, of a transition, i, between the energy levels i' and i'' is given by Eq. [2.2]. Each element of an eigenvector can be expressed in terms of its real (Re) and imaginary (Im) parts:

$$|\Phi_{i'}\rangle_k = \text{Re}|\Phi_{i'}\rangle_k + \text{Im}|\Phi_{i'}\rangle_k. \quad [II.1]$$

A term on the right-hand side of Eq. [2.2] can be expressed, for example, as

$$|\langle\Phi_{i'}|B_1S_x|\Phi_{i''}\rangle|^2 = B_1^2[\{\mathrm{Re}\langle\Phi_{i'}|S_x|\Phi_{i''}\rangle\}^2 + \{\mathrm{Im}\langle\Phi_{i'}|S_x|\Phi_{i''}\rangle\}^2] = B_1^2[\{\mathrm{ReTr}[S_x(|\Phi_{i''}\rangle\otimes\langle\Phi_{i'}|)]\}^2 + \{\mathrm{Im\ Tr}[S_x(|\Phi_{i''}\rangle\otimes\langle\Phi_{i'}|)]\}^2]. \quad [II.2]$$

In Eq. [II.2], Tr is the trace of a matrix and $|\Phi_{i''}\rangle\otimes\langle\Phi_{i'}|$ represents the outer product of the two eigenvectors $|\Phi_{i'}\rangle$ and $|\Phi_{i''}\rangle$ with the matrix elements

$$(|\Phi_{i''}\rangle\otimes\langle\Phi_{i'}|)_{jk} = |\Phi_{i''}\rangle_j|\Phi_{i'}\rangle_k^*. \quad [II.3]$$

Further, taking into account the fact that S_x is a real symmetric matrix such that the only nonzero elements in the representation in which the matrix for S_z is diagonal (so that possible values for j are over the magnetic quantum number $M = S, S-1, \ldots, -(S-1), -S$) are

$$\mathrm{Re}(S_x)_{j,j+1} = \mathrm{Re}(S_x)_{j+1,j}, \quad \text{and} \quad \mathrm{Im}(S_x)_{j,k} = 0, \quad [II.4]$$

and that

$$\mathrm{Re}(|\Phi_{i''}\rangle\otimes\langle\Phi_{i'}|)_{jk} = \mathrm{Re}|\Phi_{i''}\rangle_j\mathrm{Re}|\Phi_{i'}\rangle_k + \mathrm{Im}|\Phi_{i''}\rangle_j\mathrm{Im}|\Phi_{i'}\rangle_k$$
$$\mathrm{Im}(|\Phi_{i''}\rangle\otimes\langle\Phi_{i'}|)_{jk} = -\mathrm{Re}|\Phi_{i''}\rangle_j\mathrm{Im}|\Phi_{i'}\rangle_k + \mathrm{Im}|\Phi_{i''}\rangle_j\mathrm{Re}|\Phi_{i'}\rangle_k. \quad [II.5]$$

One obtains

$$\mathrm{Re\ Tr}[S_x(|\Phi_{i''}\rangle\otimes\langle\Phi_{i'}|)] = \sum_j (S_x)_{j,j+1} \times \{\mathrm{Re}(|\Phi_{i''}\rangle\otimes\langle\Phi_{i'}|)_{j+1,j} + \mathrm{Re}(|\Phi_{i''}\rangle\otimes\langle\Phi_{i'}|)_{j,j+1}\} \quad [II.6]$$

$$\mathrm{Im\ Tr}[S_x(|\Phi_{i''}\rangle\otimes\langle\Phi_{i'}|)] = \sum_j (S_x)_{j,j+1} \times \{\mathrm{Im}(|\Phi_{i''}\rangle\otimes\langle\Phi_{i'}|)_{j+1,j} + \mathrm{Im}(|\Phi_{i''}\rangle\otimes\langle\Phi_{i'}|)_{j,j+1}\}. \quad [II.7]$$

In Eqs. [II.6] and [II.7] the j sum is over the M values $-S, -(S-1), \ldots, (S-1)$. Thus, the right-hand side of Eq. [II.2] can be calculated by the use of Eqs. [II.6] and [II.7]. Similarly, for the B_1S_y and B_1S_z terms on the right-hand side of Eq. [2.2], one has an equation similar to Eq. [II.2] with S_x replaced by S_y and S_z, respectively.

To evaluate the corresponding expression in S_y, one notes that S_y contains only imaginary elements with the nonzero elements

$$\mathrm{Im}(S_y)_{j,j+1} = -\mathrm{Im}(S_y)_{j+1,j}$$

and

$$\mathrm{Re}(S_y)_{jk} = 0. \quad [II.8]$$

One then obtains

$$\mathrm{Re\ Tr}[S_y(|\Phi_{i''}\rangle\otimes\langle\Phi_{i'}|)] = -\sum_j \mathrm{Im}(S_y)_{j,j+1}\mathrm{Im}(|\Phi_{i''}\rangle\otimes\langle\Phi_{i'}|)_{j+1,j} \quad [II.9]$$

$$\mathrm{Im\ Tr}[S_y(|\Phi_{i''}\rangle\otimes\langle\Phi_{i'}|)] = \sum_j \mathrm{Im}(S_y)_{j,j+1}\mathrm{Re}(|\Phi_{i''}\rangle\otimes\langle\Phi_{i'}|)_{j+1,j}. \quad [II.10]$$

In Eqs. [II.9] and [II.10] the required imaginary and real parts of the outer products on the right-hand sides are gives by Eq. [II.5]. As for the corresponding expression in S_z, one notes that S_z has only diagonal elements nonzero, which are real, thus,

$$\mathrm{Im}(S_z)_{jk} = 0$$
$$\mathrm{Re}(S_z)_{jk} = (S_z)_{jk}\delta_{jk}, \quad [II.11]$$

where δ_{jk} is the Kronecker-δ symbol, such that $\delta_{ij} = 0$ for $i \neq j$, $\delta_{ij} = 1$ for $i = j$. Finally,

$$\mathrm{Re\ Tr}[S_z(|\Phi_{i''}\rangle\otimes\langle\Phi_{i'}|)] = \sum_j (S_z)_{j,j}\{\mathrm{Re}|\Phi_{i''}\rangle_j\mathrm{Re}|\Phi_{i'}\rangle_j + \mathrm{Im}|\Phi_{i''}\rangle_j\mathrm{Im}|\Phi_{i'}\rangle_j\} \quad [II.12]$$

$$\mathrm{Im\ Tr}[S_z(|\Phi_{i''}\rangle\otimes\langle\Phi_{i'}|)] = \sum_j (S_z)_{j,j}\{-\mathrm{Re}|\Phi_{i''}\rangle_j\mathrm{Im}|\Phi_{i'}\rangle_j + \mathrm{Im}|\Phi_{i''}\rangle_j\mathrm{Re}|\Phi_{i'}\rangle\}. \quad [II.13]$$

When the orientation of the $\mathbf{B}_1$ field responsible for inducing transitions is parallel to any one of the x, y, z directions, one can use the appropriate expression similar to Eq. [II.2] to calculate the relative intensity of the $i' \leftrightarrow i''$ transition. For an arbitrary orientation of the $\mathbf{B}_1$ field, one can sum the real and imaginary parts of the three terms together. The required square of the absolute value in Eq. [2.2] is then obtained as

$$|\langle\Phi_{i'}|B_{1x}S_x + B_{1y}S_y + B_{1z}S_z|\Phi_{i''}\rangle|^2 = B_1^2[|\sum_{\alpha=x,y,z} a_\alpha\mathrm{Re}\{S_\alpha(|\Phi_{i''}\rangle\otimes\langle\Phi_{i'}|)\}|^2 + |\sum_{\alpha=x,y,z} a_\alpha\mathrm{Im}\{S_\alpha(|\Phi_{i''}\rangle\otimes\langle\Phi_{i'}|)\}|^2]. \quad [II.14]$$

In Eq. [II.14], $a_x = \sin\theta\cos\varphi$, $a_y = \sin\theta\sin\varphi$, and $a_z = \cos\theta$.

APPENDIX III

Strategies to Handle Crossing and Looping Transitions

To this end, a knowledge of angular variation of B_r in a single crystal as outlined in (*2*) is helpful. The details for the two cases are as follows.

(i) Crossing transitions. When resonant fields for two transitions cross each other in such a way that the crossing takes place at one of the (θ_j, φ_j) values chosen for computation of the resonant field (case of degeneracy), only one initial value becomes available for computation of the two resonant field values at the next value $(\theta_{j+1}, \varphi_{j+1})$. This can be remedied by reducing the interval between (θ_j, φ_j) and $(\theta_{j-1}, \varphi_{j-1})$, so that degeneracy at (θ_j, φ_j) does not occur. Alternatively, one may use the perturbation expressions, or brute-force method, by diagonalizing the SH matrix for **B** values over an extended range at small intervals to find the resonant field values at $(\theta_{j+1}, \varphi_{j+1})$.

(ii) Looping transitions. There are some transitions which do not continue over all (θ_j, φ_j) values. Thus, they constitute closed curves in the (θ_j, φ_j) space on the unit sphere. Equivalently, there exist two resonant field values for the same transitions for some (θ_j, φ_j) values, while there exists no resonant field value for a transition for certain (θ_j, φ_j) values. The existence of these looping transitions can be checked by calculating resonant field values for a certain orientation (θ_0, φ_0) for which they exist. The resonant field values so obtained can then be used to calculate their angular variation by decreasing and increasing (θ_j, φ_j) in small steps form (θ_0, φ_0) until the two converge to the same value, beyond which their calculated values by the use of Eq. [3.1] become negative (*2*).

ACKNOWLEDGMENTS

The author is grateful to the Natural Sciences and Engineering Research Council of Canada for partial financial support (Grant OGP0004485) and to Dr. S. Isber for assistance in preparing the manuscript. He is particularly indebted to Professor Jack Freed of Cornell University, Ithaca, for encouraging him to develop a computer diagonalization procedure to simulate powder spectrum and providing him with the opportunity of a sojourn of 3 months in his laboratory during his sabbatical leave and continued use of his workstation "Skeeve," as well as the facilities of Cornell University Theory Center. Thanks are due to Dr. B. Lynch for providing the experimental spectrum exhibited in Fig. 2. Helpful comments on the manuscript by Professor H. Buckmaster are gratefully appreciated.

REFERENCES

1. G. H. Reed and G. D. Markham, *in* "Biological Magnetic Resonance" (L. J. Berliner and J. Reuben, Eds.), Plenum, New York), Vol. 6, pp. 73–142 (1984); More references on metalloproteins: B. Chiswell, E. D. McKenzie, and L. F. Lindboy, *in* "Comprehensive Coordination Chemistry" (G. Wilkinson, R. D. Gillard, and J. A. McCleverty, Eds.), Pergamon, Oxford, Vol. 4, pp. 1–122 (1987). For EPR crystallography of metalloproteins, see J. C. W. Chien and L. C. Dickinson, *in* "Biological Magnetic Resonance" (L. J. Berliner and J. Reuben, Eds.), Plenum, New York, Vol. 3, pp. 155–210 (1981); for ESR of iron proteins, see T. D. Smith and J. R. Pilbrow, *in* "Biological Magnetic Resonance" (L. J. Berliner and J. Reuben, Eds.), Plenum, New York, Vol. 2, pp. 85–153 (1980); for X- and Q-band EPR study of Cu^{2+}, VO^{2+}, and Gd^{3+} ions in bovine α-lactalbumin complexes, see G. Musci, G. H. Reed, and L. Berliner, *J. Inorg. Biochem.* **26,** 229 (1986); J. F. Boas, Electron paramagnetic resonance of copper proteins, *in* "Copper Proteins and Copper Enzymes" (R. Lontie, Ed.), CRC Press, Boca Raton, FL, Vol. 1, p. 6 (1984); H. Beinert, Electron paramagnetic resonance in biochemistry: Past, present and future, *Biochem. Soc. Trans.* **13,** 542 (1985); G. Palmer, The electron paramagnetic resonance of metalloproteins, *Biochem. Soc. Trans.* **13,** 548 (1985); G. R. Hanson and J. R. Pilbrow, Metalloproteins, *in* "Electron Spin Resonance" (M. C. R. Symons, Ed.), Royal Chem. Soc., London, Vol. 10B, p. 93 (1987); W. E. Blumberg and J. Peisach, Paramagnetic resonance studies of copper proteins, *Life Chem. Rep.* **5,** 5 (1987); G. R. Hanson and G. L. Wilson, Metalloproteins, *Electron Spin Reson.* **11B,** 209 (1988); J. J. Villafranca and F. M. Raushel, NMR and EPR investigations of bimetalloenzymes, *Adv. Bio-Inorg. Chem.* **4,** 289 (1990).

2. S. K. Misra and V. Vasilopoulos, *J. Phys. C: Condens. Matter* **13,** 1083 (1983).

3. M. Oettli, "The Homotopy Method Applied to Eigenvalue Problems," Technical Report 205, Department Informatik, ETH, Zurich, Dec. 1993; T. Y. Li and R. H. Rhee, Homotopy algorithm for symmetric eigenvalue problems, *Number Methods* **55** (1989); K. E. Gates, M. Griffin, G. R. Hanson, and K. Burrage, paper presented at the Rocky Mountain Conference, EPR Symposium, Denver, CO, p. 265, August 3–7 (1997). (The author is grateful to Drs. Gates and Hanson for pointing out this term.)

4. D. Wang and G. R. Hanson, *Appl. Magn. Reson.* **11,** 401 (1996).

5. D. Wang and G. R. Hanson, *J. Magn. Reson. A* **117,** 1 (1995).

6. (a) M. J. Nilges, Ph.D. Thesis, University of Illinois, Urbana, IL (1979); (b) R. L. Belford and M. J. Nilges, "Computer Simulation of Powder Spectra," EPR Symposium, 21st Rocky Mountain Conference, Denver, CO (1979); (c) A. M. Maurice, Ph.D. Thesis, Univ. of Illinois, Urbana, IL (1980).

7. S. K. Misra, *Appl. Magn. Reson.* **10,** 193 (1996).

8. W. B. Lynch, R. S. Boorse, and J. H. Freed, *J. Am. Chem. Soc.* **115,** 10909 (1993).

9. S. K. Misra, *Physica B* **240,** 183 (1997).

10. W. H. Press, S. A. Teukolsky, W. T. Vetterling, and B. P. Flannery, "Numerical Recipes in Fortran," 2nd ed., pp. 456–462, Cambridge Univ. Press (1992). The details of JACOBI subroutine, which diagonalizes a $n \times n$ real symmetric, are described in this book. It is noted that the algorithm given for the JACOBI subroutine in this book contains an error. The correct JACOBI subroutine is available at http://netlib2.cs.utk.edu/. The technique of using a real symmetric matrix to find the eigenvalues and eigenvectors of a complex Hermitian matrix, $\mathbf{A} + i\mathbf{B}$, by constructing a $2n \times 2n$ symmetric matrix using the real and imaginary parts of the SH matrix, $\begin{pmatrix} \mathbf{A} & -\mathbf{B} \\ \mathbf{B} & \mathbf{A} \end{pmatrix}$, is described on p. 475 [see also, S. K. Misra, *Magn. Reson. Rev.* **10,** 285 (1986)]. [The eigenvalues of the $2n \times 2n$ matrix are degenerate in n pairs; each pair has the eigenvalues of the matrix $\mathbf{A} + i\mathbf{B}$, and the eigenvectors (in columns with $2n$ elements) corresponding to any pair are such that the sets of upper and lower n elements can be chosen to be, respectively, the real and imaginary parts of the corresponding eigenvalue of the matrix $\mathbf{A} + i\mathbf{B}$, such that $(\mathbf{A} + i\mathbf{B})(\mathbf{u} + i\mathbf{v}) = \lambda(\mathbf{u} + i\mathbf{v})$ leads to $\begin{pmatrix} \mathbf{A} & -\mathbf{B} \\ \mathbf{B} & \mathbf{A} \end{pmatrix}\begin{pmatrix} \mathbf{u} \\ \mathbf{v} \end{pmatrix} = \lambda\begin{pmatrix} \mathbf{u} \\ \mathbf{v} \end{pmatrix}$ and $\begin{pmatrix} \mathbf{A} & -\mathbf{B} \\ \mathbf{B} & \mathbf{A} \end{pmatrix}\begin{pmatrix} -\mathbf{v} \\ \mathbf{u} \end{pmatrix} = \lambda\begin{pmatrix} -\mathbf{v} \\ \mathbf{u} \end{pmatrix}$].

11. S. K. Misra, *J. Magn. Reson.* **23,** 403 (1976).